第 6 卷　第 4 期　　航空动力学报　　Vol.6　No.4
1991 年　10 月　　Journal of Aerospace Power　　Oct.　1991

桨毂动力特性的数值模拟与实验模态分析

北航螺旋桨研究发展中心　　李可东　杜兵劳

【摘要】　桨毂动力特性用八节点三维等参元与子空间迭代法进行数值模拟；进行了实验模态分析，从而确定了桨毂前六阶的固有频率及其对应的振型。

一、数值模拟的模型及结果

飞机螺旋桨桨毂的几何形体非常复杂，孔腔结构组成大小不一，转接半径曲率各异。必须做许多形体上的简化，离散为有限个单元，形成一多自由度振动系统，才能进行近似的数值模拟。对于这样复杂的形体，在建立计算模型时，考虑到计算结果的准确性、可用性，我们按三维等参元概念采用了八节点任意六面体单元。整个桨毂划分为 616 个单元，总节点数达 1236 个。即使这样由于系统的自由度已近 4000，致使编制的程序，运行时容量已需 8 兆。如果再将网格分细，或将单元节点增多，计算会更繁复。因此，为了综合协调各方面因素，特别是实际应用的需要，我们确定数值模拟的目标为：(1) 能反映复杂形体结构动力特性的特点，即振频的密集性；(2) 能划出一条最低固有频率的界限，以判别对桨毂的实际工作是否允许；(3) 能为实验模态分析定出数量级概念。多自由度无阻尼自由振动方程为

$$[M]\{\ddot{\delta}\} + [K]\{\delta\} = \{0\} \tag{1}$$

其中 $\{\delta\}$ 为系统的节点位移，可见分析系统的振动特性，必须从总体质量矩 $[M]$ 与总体刚度矩阵 $[K]$ 入手。设三维等参元的局部坐标为 ξ, η, ζ 则单元刚度矩阵

$$[K_{ij}]^e = \int_{-1}^{1}\int_{-1}^{1}\int_{-1}^{1}[B_i]^T[D][B_j]\,|J|\,d\xi d\eta d\zeta \tag{2}$$

(2) 式通常是用高斯公式求积。为协调刚度矩阵的误差，各向取两个积分点，即得

$$[K_{ij}]^e \cong \sum_{i_1=1}^{2}\sum_{i_2=1}^{2}\sum_{i_3=1}^{2}([B_i]^T[D][B_j]|J|)H_{i1}H_{i2}H_{i3} \tag{3}$$

按 Legendre 多项式，得出单元内三向的八个积分点为：

$$f(1/\sqrt{3}, 1/\sqrt{3}, 1/\sqrt{3}),\quad f(1/\sqrt{3}, 1/\sqrt{3}, -1/\sqrt{3}),$$
$$f(1/\sqrt{3}, -1/\sqrt{3}, 1/\sqrt{3}),\quad f(1/\sqrt{3}, -1/\sqrt{3}, -1/\sqrt{3}),$$
$$f(-1/\sqrt{3}, 1/\sqrt{3}, 1/\sqrt{3}),\quad f(-1/\sqrt{3}, 1/\sqrt{3}, -1/\sqrt{3}),$$
$$f(-1/\sqrt{3}, -1/\sqrt{3}, 1/\sqrt{3}),\quad f(-1/\sqrt{3}, -1/\sqrt{3}, -1/\sqrt{3})。$$

加权系数 $H_{i1} = H_{i2} = H_{i3} = 1$。雅可比行列式 $|J|$ 按雅可比矩阵

$$[J] = \begin{bmatrix} \partial N_1/\partial\xi & \partial N_2/\partial\xi & \cdots & \partial N_8/\partial\xi \\ \partial N_1/\partial\eta & \partial N_2/\partial\eta & \cdots & \partial N_8/\partial\eta \\ \partial N_1/\partial\zeta & \partial N_2/\partial\zeta & \cdots & \partial N_8/\partial\zeta \end{bmatrix} \begin{bmatrix} X_1 & Y_1 & Z_1 \\ X_2 & Y_2 & Z_2 \\ \vdots & \vdots & \vdots \\ X_8 & Y_8 & Z_8 \end{bmatrix} \tag{4}$$

求得。在划分单元时, 各节点的坐标 X、Y、Z 已经定出, 八节点三维等参元的形函数为

$$N_i(\xi,\eta,\zeta) = (1+\xi_i\xi)(1+\eta_i\eta)(1+\zeta_i\zeta)/8 \tag{5}$$

故可算出 $[J]$。(3) 式中

$$[B] = \begin{bmatrix} \partial N_i/\partial X & 0 & 0 \\ 0 & \partial N_i/\partial Y & \\ 0 & 0 & \partial N_i/\partial Z \\ \partial N_i/\partial Y & \partial N_i/\partial X & 0 \\ 0 & \partial N_i/\partial Z & \partial N_i/\partial Y \\ \partial N_i/\partial Z & 0 & \partial N_i/\partial X \end{bmatrix} \tag{6}$$

矩阵中的元素

$$[\partial N_i/\partial X \quad \partial N_i/\partial Y \quad \partial N_i/\partial Z]^T = [J]^{-1}[\partial N_i/\partial\xi \quad \partial N_i/\partial\eta \quad \partial N_i/\partial\zeta]^T \tag{7}$$

故按桨毂材料的弹性模量 E 和波松比 μ 求定弹性矩阵 $[D]$ 后, 即可计算单元刚度矩阵 $[K]^e$。单元质量矩阵在等参元内对局部坐标进行积分为

$$[M]^e = \int_{-1}^{1}\int_{-1}^{1}\int_{-1}^{1} \rho [N]^T[N]|J| d\xi d\eta d\zeta \tag{8}$$

应用前面相同的数值方法, 表示为

$$[M]^e \cong \sum_{i_1=1}^{2}\sum_{i_2=1}^{2}\sum_{i_3=1}^{2} (\rho[N]^T[N]|J|) H_{i1}H_{i2}H_{i3} \tag{9}$$

式中 ρ 为桨毂材料密度; $[N]$ 为形函数矩阵。

$$[N]^T[N] = \begin{bmatrix} N_1^2 & 0 & 0 & N_1N_2 & 0 & \cdots & N_1N_8 & 0 & 0 \\ 0 & N_1^2 & 0 & 0 & N_1N_2 & & 0 & N_1N_8 & 0 \\ 0 & 0 & N_1^2 & 0 & 0 & & 0 & 0 & N_1N_8 \\ N_2N_1 & 0 & 0 & N_2^2 & 0 & & N_2N_8 & 0 & 0 \\ 0 & N_2N_1 & 0 & 0 & N_2^2 & & 0 & N_2N_8 & 0 \\ 0 & 0 & N_2N_1 & 0 & 0 & & 0 & 0 & N_2N_8 \\ \vdots & \vdots & \vdots & \vdots & \vdots & & \vdots & \vdots & \vdots \\ N_8N_1 & 0 & 0 & N_8N_2 & 0 & & N_8^2 & 0 & 0 \\ 0 & N_8N_1 & 0 & 0 & N_8N_2 & & 0 & N_8^2 & 0 \\ 0 & 0 & N_8N_1 & 0 & 0 & & 0 & 0 & N_8 \end{bmatrix} \tag{10}$$

为一满矩阵, 这对存贮和运算, 都将造成很大的困难。

但我们看到对角线元素为 N_i^2, 如果只计算对角线元素, 则为

$$m_{ii} \cong \sum_{i_1=1}^{2}\sum_{i_2=1}^{2}\sum_{i_3=1}^{2} (\rho N_i^2|J|) H_{i1}H_{i2}H_{i3} \tag{11}$$

$|J|$ 沿单元积分即为单元之体积，令为 J_T，则 $\rho J_T = TM$ 为单元之质量。将 N_i^2 积分后，令为 $EMM(i)$，将质量按

$$m_{ii} = TM \cdot EMM(i) \Big\backslash \sum_{i=1}^{8} EMM(i) \qquad (i = 1, 2, \cdots, 8) \tag{12}$$

分配到八个节点上，而得一单元集中质量矩阵 $[M]^e$，这样便使运算简化多了。

在 (1) 式中如果系统自由振动的频率为 ω，则

$$\delta_i = X_i \sin\omega t \qquad (i = 1, 2, \cdots n) \tag{13}$$

Y_i 为振幅，代入 (1) 式得

$$-\omega^2[M]\{X_i\} + [K]\{X_i\} = \{0\} \tag{14}$$

则特征方程为

$$\det\left|[K] - \omega^2[M]\right| = 0 \tag{15}$$

系统的总刚度矩阵 $[K]$ 与总质量矩阵 $[M]$ 由前述单元质量矩阵与单元刚度矩阵组集而成为 $n \times n$ 阶。如果按接近4000 的自由度来计算固有频率, 不仅运算十分浩繁, 而实际上又不需要。如果能算出浆毂前 16 阶振动特性，已绰绰有余了。为了得到前 16 阶较为精确的结果，按经验应计算的阶数 q 有 $q/2+1=16$，所以 $q=30$。由此可见，对 (14) 式，应进行降阶处理。我们假定 q 个独立矢量 $\{Y_i\}$ ($i=1, 2, \cdots, q$) 的线性组合为振型 $\{X\}$，即

$$\underset{nxl}{\{X_i\}} = \underset{n\times q}{[Y]}\ \underset{q\times l}{\{A\}} \tag{16}$$

$\{A\}$ 为一待定系数列阵。并可写出

$$[Y]^T[K][Y]\{A\} - \omega^2[Y]^T[M][Y]\{A\} = \{0\} \tag{17}$$

令

$$\underset{q\times n}{[Y]}^T \underset{n\times n}{[K]}\ \underset{n\times q}{[Y]} = \underset{qxq}{[K]}^*, \qquad \underset{q\times n}{[Y]}^T \underset{n\times n}{[M]}\ \underset{n\times q}{[Y]} = \underset{q\times q}{[M]}^* \tag{18}$$

则 (17) 式的特征方程为

$$\det\left|[K]^* - \omega^2[M]^*\right| = 0 \tag{19}$$

可见已将一个 $n\times n$ 阶矩阵特征值问题缩减为 $q\times q$ 阶矩阵特征值问题。$q \ll n$，故使计算简化。

算出前 q 阶固有频率 ω_1，ω_2，$\cdots$，ω_q 后，依次代入 (17) 式，即可算出各阶特征向量 $\{A_j\}$ ($j=1, 2, \cdots q$)，再由 (16) 式求出前 q 阶近似主振型。

由于初始振型 $\{X\}$ 是假设的故必须通过迭代，算准振型求得的频率 ω 才准确。

刚度矩阵是在浆毂自由支承状态下求得的，是半正定的无法求逆。我们用"移频"方法求得的结果很不合理，才改用固定 32 个节点的方法计算前 30 阶特性。从计算机输出的前 16 阶数据中，经过分析，得出浆毂前六阶的固有频率见表 1。

表 1　梁毂前六阶的固有频率

频率阶次	1	2	3	4	5	6
数值 Hz	1121	1580	2879	3134	3405	4136

由算得的结果看，固有频率是较为密集的，能反映复杂形体件振动特点。最低频率为 1121Hz。这些数据为实验模态分析提供了基础。

二、实验模态分析设备与测点安排

实验模态分析设备与安排如图 1。浆毂用锤击激振，传感器附于锤头上。加速度传感器粘结在浆毂测试点上拾振。两个电荷放大器，使传感器传来的激振力信号和振动位移信号增益, 然后输入 7T 17S 信号处理仪。应用该机所附 Modal No. 1 软件进行模态分析。在 7T 17S 的屏幕上可以显示分析数据和图形，并可用热印机打印下来，以便分析。经反复调试，最后

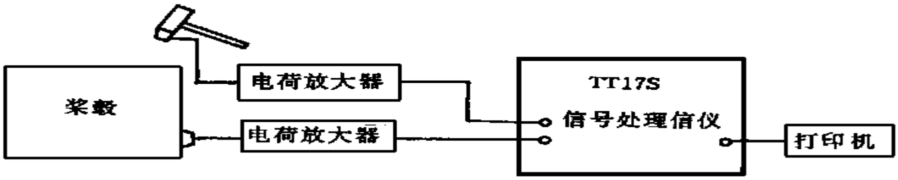

图 1 设备图

确认机器提供的桨毂各阶固有频率和振型。按多自由度振动微分方程

$$[M]\{\ddot{X}\} + [C]\{\dot{X}\} + [K]\{X\} = \{F\} \tag{20}$$

应用比例粘性概念解耦，并以模态坐标 $\{q\}$ 取代物理坐标 $\{X\}$，即

$$\{X\} = \sum_{r=1}^{n} q_r\{\varphi\}_r = [\Phi]\{q\} \tag{21}$$

$[\Phi]$ 为特征向量矩阵。写出任意第 r 个方程

$$m_r\ddot{q}_r + c_r\dot{q}_r + k_r q_r = \{\varphi\}_r^T\{F\} \tag{22}$$

其中 m_r、c_r、k_r 和 $\{\varphi\}_r^T\{F\}$ 即分别为模态质量、模态阻尼、模态刚度和模态力列阵。

将 (22) 式进行 Raplace 变换，有

$$(-\omega^2 m_r + j\omega c_r + k_r)\, q_r(j\omega) = \{\varphi\}\{F(j\omega)\} \tag{23}$$

故得

$$q_r = (\{\varphi\}_r^T\{F\})/(-\omega^2 m_r + j\omega c_r + k_r) \tag{24}$$

q_r 和 F 都是频域变量。代回 (21) 式，有

$$\{X\} = \sum_{r=1}^{n}\frac{\{\varphi\}_r^T\{F\}\{\varphi\}_r}{-\omega^2 m_r + j\omega c_r + k_r} = \sum_{r=1}^{n}\frac{\{\varphi\}_r\{\varphi\}_r^T}{-\omega^2 m_r + j\omega c_r + k_r}\{F\} \tag{25}$$

则

$$X_i = \sum_{r=1}^{n}\frac{1}{-\omega^2 m_r + j\omega c_r + k_r}(\varphi_{ir}\varphi_{1r}F_1 + \varphi_{ir}\varphi_{2r}F_2 + \cdots + \varphi_{ir}\varphi_{jr}F_j + \cdots + \varphi_{ir}\varphi_{nr}F_n) \tag{26}$$

故由激振力 F_j 产生的响应

$$X_{ij} = \sum_{r=1}^{n}\frac{\varphi_{ir}\varphi_{jr}}{-\omega^2 m_r + j\omega c_r + k_r}\cdot F_j \tag{27}$$

按传递函数概念，可以写出

$$H_{ij} = \frac{X_{ij}}{F_j} = \sum_{r=1}^{n}\frac{\varphi_{ir}\varphi_{jr}}{-\omega^2 m_r + j\omega c_r + k_r} = \sum_{r=1}^{n}\frac{\varphi_{ir}\varphi_{jr}/m_r}{-\omega^2 + \omega_r^2 + j2\zeta_r\omega_r\omega} \tag{28}$$

式中 $\omega_r = \sqrt{k_r/m_r}$，$\zeta_r = c_r/2\sqrt{m_r k_r}$，(27) 式和 (28) 式给予我们一个重要的启示，在进行模态分析时，不管是怎样的激振力 F_j，总可在振动体上获得一响应 X_{ij}，而且 φ_{jr}就是激振点的幅值，φ_{ir}就是响应点的幅值，H_{ij}就是在 j 点激振，i 响应点的传递函数。

由 (28) 式看出，反映固有频率的分母，与激振点、响应点 i、j 无关，故求桨毂的固有频率，只测一个传递函数即可。而求振型则需测出能反映振动特征的各点的传递函数。由于桨毂形体十分复杂，要满足这一要求，至少也要 80 个测点提供信号。而 7T17S 的模态分析软件最多只能做 127 个传递函数。因为要反映三维振型，就只能处理 42 个测试点的信号。

桨毂的宏观外形，可以粗略视为三个圆筒相贯而成，因此我们采用了分区逐次测试的方法。四个安装桨叶的桨轴，振型基本相同，对其中一个安排 31 个测点，如图 2a；后面与桨轴相连的轴向小端，与前面的和变矩油缸相连的大端比，振幅较小，测定意义不大，故只在大

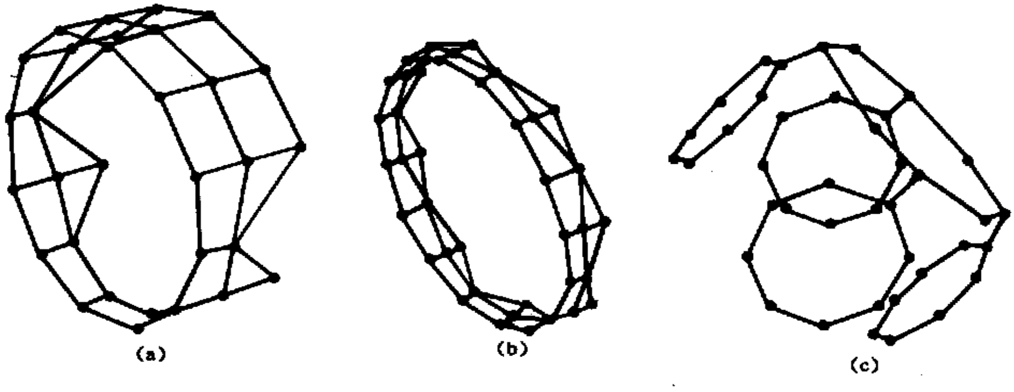

图 2　测点分布

端大安排了 40 个测点，如图 2b；为了说明各部分振型的相对关系，又在总体上安排了 40 个测点，如图 2c，然后分三次测试。

三、测试结果及分析

由于桨毂形体复杂，敲击不便，故采用固定激振点移动响应点的方法来测取传递函数。

将激振与响应信号输入 7T17S 处理仪，经 A/D 转换和 FFT 变换，即得传递函数。由于数据只能有限采集，所得传递函数为等频间隔的离散数据，故须进行曲线拟合，即在等距间隔数据间进行插值计算，以求得完整的传递函数曲线，显示精确的峰值和固有频率。图 3 即

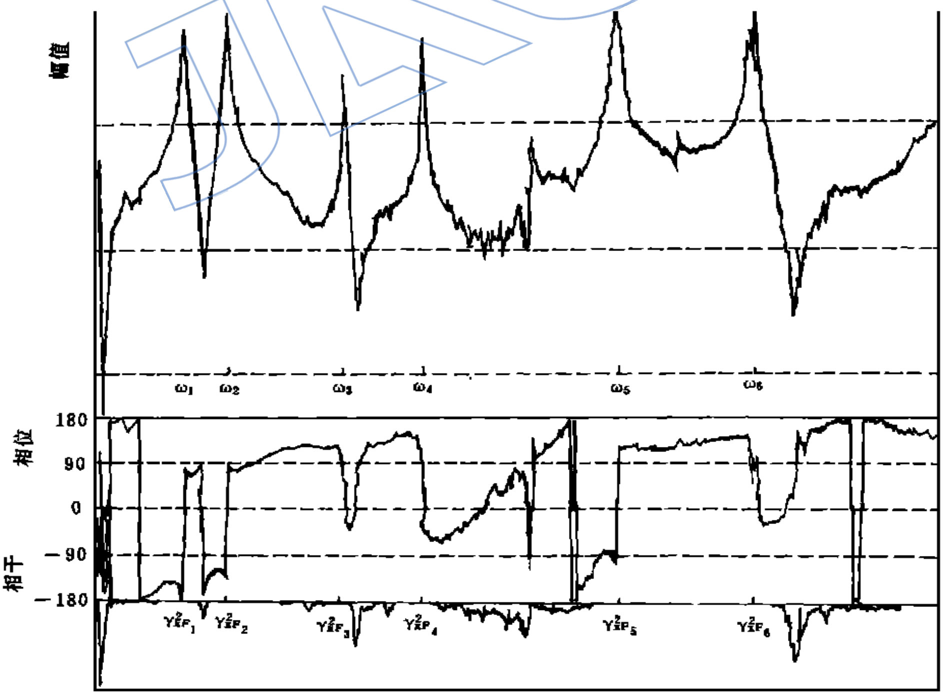

图 3　幅频 · 相频图

为测出的幅频·相频图。从图上可以看到桨毂前6阶的固有频率，其所对应的相干函数均为1，说明所得传递函数是可用的。

邻近某阶固有频附近取一区段，按测得的传递函数等频间隔取其虚、实部值，作为一个数值点，以小方块表示，如图4，至少取7点，称做Nyquist图。在固有频率附近，Nyquist图理论为一圆。从图上观察，实测的8点，确实在圆的附近，说明所测的传递函数是很好的。

桨毂前六阶固有频率对应的振型均分三次测出，测得的前六阶固有频率见表2。

表2 前六阶固有频率

频率阶次	1	2	3	4	5	6
数值Hz	1783	1885	2045	2208	2342	2594

与表1对比，固有频率更趋密集，在数量级是对应的，但有误差。存在误差是网格不能再细分，带来有限元法的固有近似性；其次是高斯积分点较少，非等量分布的集中质量矩阵以及固定节的位置选取未必合适，使对桨毂刚性的模拟发生误差；另外，为了减少计算机时，程序采用了单精度数，增大舍入误差。但数值模拟对实验结果起到了应有的映证作用。

为了进一步考查实验结果的可靠性，又用相同实验方法和相同模态分析设备对一有解析解的钢质圆环进行了实测，取得的结果见表3。

表3 实验频率与计算频率比较

振型及阶次	实验频率(Hz)	计算频率(Hz)	误差(%)
一阶面内弯曲	284	283	0.4
二阶面内弯曲	799	800	0.1
三阶面内弯曲	1497	1534	2.5

从表上可以看出实验结果相当精确，说明所用模态分析设备是可靠的，实验方法是成功的，所得结果是可信的。

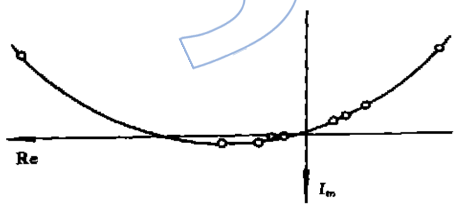

图4 Nyquist图

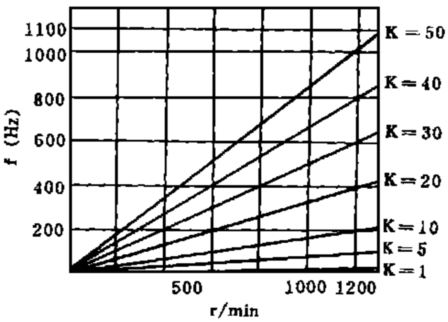

图5 共振特性图

结论 本文研究的目的，在于判断桨毂在动力特性方面是否能可靠工作。为此必须画出共振特性图。以桨毂的工作转速为横坐标轴，振动频率为纵坐标轴，如图5。桨毂实验的最低固有频率为1783Hz，为可靠起见，按计算的最低频率1100Hz画出桨毂的自振频率线。由于桨毂刚性较高转速较低，不计动频差异则为一等频线。按转速的一倍($K=1$)、五倍($K=5$)等等画出桨毂的激振频率线。激振频率线与自振频率线的交点对应的转速，即共振转速。对一转速为1245r/min的桨毂，即使激振频率为转速的50倍，图上还无交点，即桨毂在工作转速范围内不致产生共振。这说明桨毂在动力特性方面的设计是符合要求的，桨毂是安全可用的。

(责任编辑 朱梓根)

AEROACOUSTICAL MODIFICATION OF A PROPELLER

Li Xiaodong, Yang Xiaodong, Hu Zongan (*APRDC, BUAA*)

ABSTRACT An aeroacoustical modification of a propeller is considered with the aim of great enhancement of its takeoff efficiency and appropriate cutdown of its noise level when its blade number, blade hub and cruise efficiency are kept unchanged. A time domain method is applied to predicting near and far the sound field. From iterative aeroacoustical and aerodynamical optimization an optimum design scheme has been obtained. And two 1/3-scaled model propellers were made to simulate the original and modified propellers respectively. The results of comparative ground experiments show that the OASPL (Overall Sound Pressure Level) decreases by 1 to 1.5 dB while other technical spesifications are met.

EXPERIMENTAL CHARACTERISTICS COMPARISON BETWEEN TWO SCALE-MODEL PROPELLERS

Mao Xichang, Wang Jiebing, Li Hongmin (*APRDC, BUAA*)

ABSTRACT The aerodynamic and acoustic charaeteristics of two scale-model propellers are compared experimentally. A three blades model (Model A) is a scale-model of a production type. A four-blades model (Model B) is a scale-model of a new designed propeller. Their rotational speeds vary between 1500 to 3000rpm. Experimental results indicate that under identical operational conditions the four-blades propeller has higher thrust coefficient but lower noise level than the three-blades propeller and also has lower noise level at the same power coefficient. The four-blades propeller, of course, is superior to the three-blades one in the efficiency and overall performance.

STRESS ANALYSIS OF A PROPELLER BLADE

Xiong Changbing (*APRDC, BUAA*)

ABSTRACT Three-dimensional finite element method is applied to stress analysis of the original and the redesigned propeller blade taking the loads, such as centrifugal and dynamical loads. In respect of stress distribution, the airfoil of the redesigned propeller blade is more reasonable. Its stress distribution approaches to isostrength, and safety coefficient also meets the given specification. Therefore, the redesigned propeller blade is an quite advanced design.

STRESS ANALYSIS OF A PROPELLER HUB

Xiong Changbing (*APRDC, BUAA*)

ABSTRACT Three-dimensional finite element method is applied to stress analysis of a propeller hub taking centrifugal load, aerodynamical moment and blade centrifugal tension load. Since its construction is complicated, loads are various and its stress distribution is hard to analyze, the elastic stress plus principle is employed for this purpose. The analytical results show that the blade centrifugal tension load is predominant and its construction has been optimized to a certain extent due to current improvements during long time of its service and modifications so the stress distributions of its parts are quite even and reasonable, moreover safety coefficients are large enough.

DIGITAL SIMULATION AND EXPERIMENTAL MODAL ANALYSIS OF DYNAMIC CHARACTERISTICS OF A PROPELLER HUB

Li Kedong and Du Binlao (*APRDC, BUAA*)

ABSTRACT The finite element method with 8-nodes three-dimensional isoparametric elements and subspace iteration is applied to digital simulation of dynamic characteristics of a propeller hub. The sizes of the stiffness matrices [K] and mass matrices [M] in the equations are very large. The natural frequencies of the first six orders and its corresponding modes of the hub have been obtained from the experimental modal analysis. By comparison the results of the experimental modal analysis and the digital simulation are of the same order.

EXPERIMENTAL MODAL ANALYSIS OF PROPELLER BLADES

Li Qihan, Chen Zhiying, Zhang Dalin (*APRDC, BUAA*)

ABSTRACT The vibration characteristics of propeller blades have been investigated by using experimental modal analysis technique. The emphasis of the investigation is put on the effects of different joint conditions of blade root ends and mounting ways of blades on the nature frequencies and modes of propeller blade vibration. From the contrast analysis of the results it is concluded that in order to understand and analyze the dynamic characteristics of propeller blades precisely, the calculations and experiments of coupling dynamic characteristics of blade-hub-shaft of propeller assembly should be completed for simulating the joint and mounting conditions between propeller and engine practically.

VIBRATION CHARACTERISTIC ANALYSIS OF A PROPELLOR BLADE

Kong Ruilian and Wang Yanrong (*APRDC, BUAA*)

ABSTRACT The subspace iteration method and Jacobi's method are used to solve the eigenvalue problem for the vibration of a propeller blade, in which the super-parametric quadratic thick shell element with eight nodes and forty degrees of freedom is used to govern the motion equation, considering the effects of shear transverse deformation on the accuracy. The frequencies and vibration modes calculated by the program written by authors are in quite good agreement with the experimental results, and they can be used to judge whether the resonance occurs in the operation of the propeller, considering the effects of aerodynamic force excitation only.

A METHOD OF RELIABILITY ANALYSIS FOR PROPELLER BLADES

Fu Huimin and Gao Zhentong (*APRDC, BUAA*)

ABSTRACT A distribution function of two-dimensional threshold is given for fatigue crack propagation. A two-dimensional stress-threshold interference model is set up. The model is applicable to the reliability analysis and design of infinite life for propeller blades or other structural members with initial defects and accident damage. The functional correlation between the reliability of no crack growth and the initial crack sizes is obtained from the model and the maximum permissible crack sizes can be determined according to a given reliability level. In consideration of the fact, that the longer the service time, the greater the probability of accident damage, the overhaul periods of propeller blades with high reliability are also given.

EFFECT OF ANTIICER ON PROPELLER PERFORMANCE

ZhangAikun (*APRDC, BUAA*)

ABSTRACT Comparative experiments of a propeller with and without the antiicer have been completed in a wind tunnel. The analysis of the experimental data shows that the effect of the anticer depends on the advance ratio (J) and the blade angle (β). First, the antiicer has no effect on the performance of the propeller when the blade angle is big enough and the advance ratio is small ($\beta = 40°$, $J < 0.5$). Second, the efficiency of the propeller with antiicer increases when the blade angle is big enough and the J is moderate ($\beta = 40°$, $0.5 < J < 1.3$) or the blade angle is smaller and the J also small ($\beta = 27.5°$, $J < 0.5$). Third, the attached antiicer reduces effficiency at the big blade angle with a large advance ratio ($\beta = 40°$, $J > 1.3$) or at a smaller angle with a moderate ratio ($\beta = 27.5°$, $J > 0.5$). In fact, when aircraft is flying, its propeller is almost running at the third condition. When the airarft takes off ($J = 0.618$, $\beta = 28.79°$), the antiicer reduces the propeller efficiency by 1.5 percent, and by 3 percent when the plane cruises ($J = 1.6130$, $\beta = 40.41°$).